Journal of Luminescence 22 (1981) 349–358
North-Holland Publishing Company

TIME-RESOLVED SITE-SELECTION SPECTROSCOPY STUDIES OF $NdAl_3(BO_3)_4$ CRYSTALS

Dhiraj K. SARDAR and Richard C. POWELL

Physics Department, Oklahoma State University, Stillwater, Oklahoma 74078, USA

Original manuscript received 30 May 1980
Revised manuscript received 8 December 1980

A pulsed, tunable dye laser was used to selectively excite Nd^{3+} ions in nonequivalent crystal field sites in $NdAl_3(BO_3)_4$ crystals and energy transfer between ions in different types of sites was studied by monitoring the time evolution of the fluorescence spectrum. The results show that the energy transfer rate varies as $t^{-1/2}$ and increases with temperature. The predictions of various models of phonon-assisted energy transfer are compared to the results.

1. Introduction

Neodymium aluminum borate, $NdAl_3(BO_3)_4$, is one of the several "stoichiometric laser materials" which have gained recent interest due to their use in minilaser applications [1,2]. In these materials a high concentration of Nd^{3+} ions can be present (5.43×10^{21} cm^{-3} for $NdAl_3(BO_3)_4$) without strong concentration quenching of the fluorescence emission. Since these materials are relatively new, there are still many aspects of their physical properties that are not well characterized and understood.

$NdAl_3(BO_3)_4$ (NAB) has a complex crystal structure with marked deviation from inversion symmetry and significant isolation of the Nd polyhedra [3,4]. The strong odd-parity crystal field admixture of the f and d configurations results in a short radiative lifetime and the highest cross section of any Nd material. Although laser action has been observed in NAB, the spectroscopic properties of the material have not been well characterized [5,6]. One property of special interest which has not been investigated is the interaction between Nd^{3+} ions which may lead to fluorescence quenching.

We report here the results of a study of energy transfer among Nd^{3+} ions in NAB crystals. Time-resolved site-selection spectroscopy techniques were employed to determine the magnitude, time dependence, and temperature dependence of the rate of energy transfer between Nd^{3+} ions in nonequivalent types of crystal field sites. Several possible interpretations of the results are discussed.

0022-2313/81/0000–0000/$02.50

2. Experimental techniques

The samples consisted of small single crystal pieces of $NdAl_3(BO_3)_4$. These were mounted on the cold finger of a cryogenic refrigerator capable of varying the temperature from about 10 K up to room temperature. A block diagram of the experimental apparatus is shown in fig. 1. A nitrogen laser-pumped tunable dye laser was used to excite the sample. Using rhodamine 6G, a pulse of less than 10 ns in duration and about 0.4 Å halfwidth was obtained. The sample fluorescence was focused onto the entrance slit of a one-meter monchromator and detected by a cooled RCA C31034 photomultiplier tube. The signal was averaged by a boxcar integrator triggered by the laser so that either the lifetimes or the fluorescence spectra at different times after the excitation pulse could be recorded.

The wavelength of the dye laser excitation light was approximately 5920 Å which is absorbed in one of the higher excited states of the Nd^{3+} ions. After relaxation of the $^4F_{3/2}$ metastable state, the emission to the various components of the $^4I_{9/2}$ ground state manifold was monitored. The lifetime of fluorescence was found to be 20 μs and independent of temperature between 10 and 295 K.

The fluorescence spectrum of $NdAl_3(BO_3)_4$ at 11 K in the region from 8780 to 8940 Å is shown in fig. 2 for two different excitation wavelengths. The lines from each transition exhibit a significant amount of structure and the dominant structural components vary significantly with excitation wavelength. The

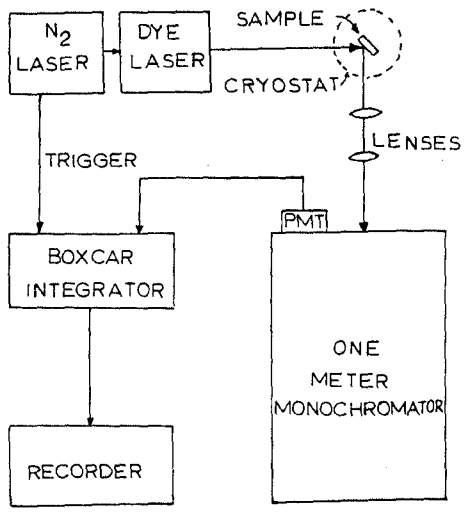

Fig. 1. Block diagram of experimental apparatus.

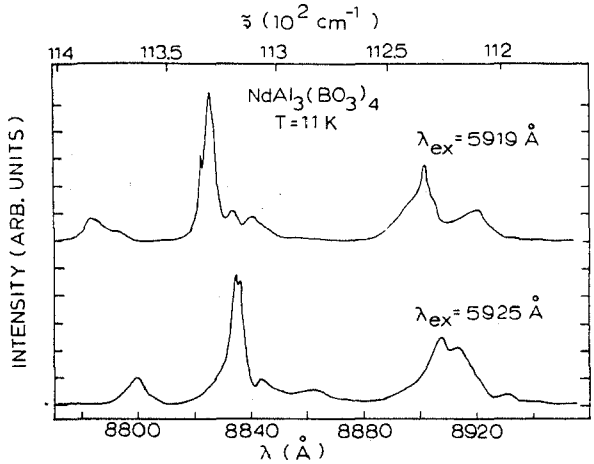

Fig. 2. Fluorescence spectra of $NdAl_3(BO_3)_4$ at 11 K for two different excitation wavelengths.

relative intensities of these peaks vary in a uniform, continuous way between the two extremes shown in fig. 2 as the laser wavelength is scanned from 5919 to 5925 Å. This structure can be attributed to the presence of ions in slightly different types of crystal field sites. By tuning the dye laser wavelength, ions in specific types of sites are selectively excited. Energy transfer between ions in spectrally different sites can be studied by monitoring the time evolution of the fluorescence spectra after the laser pulse. Fig. 3 shows the spectrum at two times after the excitation pulse for a specific excitation wavelength at low

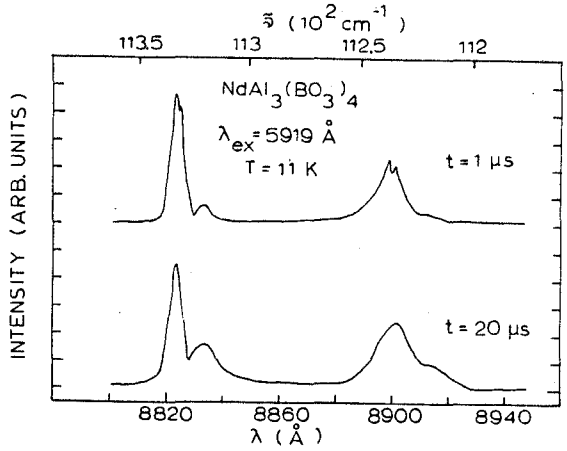

Fig. 3. Fluorescence spectra of $NdAl_3(BO_3)_4$ at 11 K at two times after the excitation pulse.

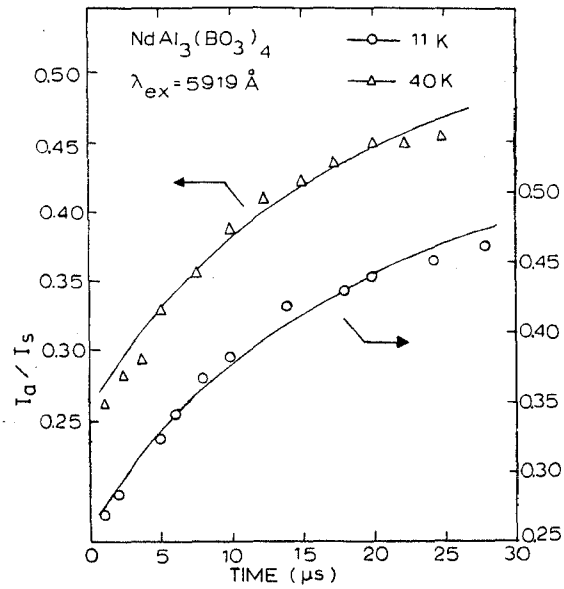

Fig. 4. Ratios of the integrated fluorescence intensities of activator and sensitizer transitions as a function of time after the excitation pulse at 11 K and 40 K. See text for explanation of theoretical lines.

temperature. At short times, the high energy components of the transitions are dominant; as time increases the low energy components grow in intensity with respect to the high energy lines.

The quantitative analysis of energy transfer from Nd^{3+} ions in sites producing the high energy transitions (sensitizers) to ions in sites resulting in the low energy transitions (activators) can be obtained by plotting the time dependence of the ratios of the integrated fluorescence intensities of the activator and sensitizer transitions. The results are shown in fig. 4 for 11 and 40 K. At higher temperatures the lines are broadened to the extent that the transitions from ions in nonequivalent sites cannot be resolved accurately. The solid lines in the figure represent theoretical fits to the data discussed in the following section.

3. Interpretation

The time-resolved spectroscopy results can be interpreted using the phenomenological rate parameter model shown in fig. 5. The "sensitizer" ions are those in the site preferentially excited by the laser at a rate W_s, whereas the

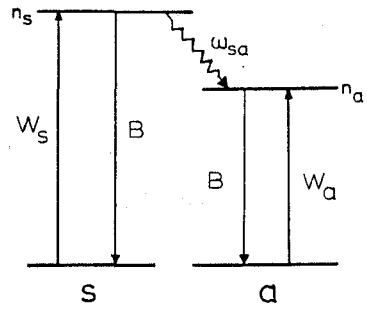

Fig. 5. Model for interpretation of energy transfer data. See text for explanation of symbols.

"activators" are ions in sites which receive the energy through energy transfer as well as being excited by the laser at a rate W_a. n_s and n_a are the concentrations of ions in the excited states, ω_{sa} is the rate of energy transfer, and B is the fluorescence decay rate which was found to be approximately the same for ions in both types of sites.

The rate equations describing the time evolution of the populations of excited states are

$$dn_s/dt = W_s - Bn_s - \omega_{sa}n_s, \tag{1}$$

$$dn_a/dt = W_a - Bn_a + \omega_{sa}n_s. \tag{2}$$

These equations can be solved assuming a delta-function excitation pulse and an explicit time dependence for the energy transfer rate. A variety of different theoretical models were tested, but it was found that the best fits to the data at both low and high temperatures were obtained with an energy transfer rate which varied as $t^{-1/2}$. The solutions of eqs. (1) and (2) are

$$n_s(t) = n_s(0)\, e^{-Bt-2\omega t^{1/2}}, \tag{3}$$

$$n_a(t) = n_s(0)\left[e^{-Bt} - e^{-Bt-2\omega t^{1/2}}\right] + n_a(0)\, e^{-Bt}, \tag{4}$$

where the time dependence of the energy and transfer rate is written explicitly as $\omega_{sa} = \omega t^{-1/2}$. The ratio of integrated fluorescence intensities is then given by

$$\frac{I_a}{I_s} = K\left\{\left(\frac{n_a(0)}{n_s(0)} + 1\right) e^{2\omega t^{1/2}} - 1\right\}, \tag{5}$$

where K is a constant containing factors including the radiative emission rates. The solid lines in fig. 4 represent the predictions of this expression treating K, ω and $n_a(0)/n_s(0)$ as adjustable parameters.

The temperature dependence of the energy transfer rate was determined by measuring the fluorescence intensities at different times after the excitation

pulse as a function of temperature and fitting the data using eq. (5). The results are shown in fig. 5. The transfer rate was found to be approximately constant below 25 K and to increase at higher temperatures.

4. Discussion and conclusions

The time dependence of the energy transfer rate is a sensitive indicator of the mechanism of energy transfer. The $t^{-1/2}$ variation observed here can be due to several types of processes: single-step electric dipole–dipole interaction between randomly distributed sensitizers and activators; multistep energy migration on a one-dimensional lattice; and trap-modulated energy migration in three dimensions. The first of these possibilities is generally the most common and can be verified through theoretical predictions of the magnitude of the energy transfer rate. At 11 K the measured value of ω is 0.16 $\mu s^{-1/2}$. The theoretical expression for the rate of single-step electric dipole–dipole energy transfer among randomly distributed ions is [7]

$$\omega_{sa} = \tfrac{4}{3}\pi^{3/2} C_a R_0^3 / (\tau_s t)^{1/2}, \tag{6}$$

where C_a is the concentration of activators, τ_s is the intrinsic fluorescence decay time of the sensitizers and the critical interaction distance is given by [8]

$$R_0 = \left[\tfrac{3}{4} \frac{e^2}{mc^2} f_a \frac{\Omega \phi_s}{(2\pi n \tilde{\nu}_{sa})^4} \right]^{1/6}, \tag{7}$$

where ϕ_s is the quantum efficiency of the sensitizer, f_a is the oscillator strength of the activator, $\tilde{\nu}_{sa}$ is the average wave number in the region of spectral overlap, and Ω is the spectral overlap integral. Using the measured value of the energy transfer rate in eq. (6) along with the values of $C_a = 1.4 \times 10^{21}$ cm^{-3} determined by comparing relative spectral intensities at different excitation wavelengths and $\tau_s = 50$ μs which is the value measured in lightly doped borate samples [9] gives a measured value of $R_0 = 3.0$ Å. This can be compared to the theoretical value predicted by eq. (7), where f_a is calculated from spectral measurements to be 2.3×10^{-4} and the overlap integral is approximated by the overlap of two Lorentzian lines

$$\Omega \approx \frac{1}{\pi} \frac{\Delta\tilde{\nu}_s + \Delta\tilde{\nu}_a}{(\Delta\tilde{\nu}_s + \Delta\tilde{\nu}_a)^2 + (\tilde{\nu}_s^0 - \tilde{\nu}_a^0)^2}. \tag{8}$$

At 11 K the predicted value is $R_0 = 7.6$ Å. The difference in the predicted and measured values of R_0 is significant. Although some of the values of the parameters used in obtaining these results are rough estimates, such as ϕ_s and Ω, any reasonable choice of values given at least a factor of 2 difference between the two determinations of R_0.

The inconsistency described above indicates that the single-step mechanism is not responsible for the observed energy transfer in this system. The second type of possible energy transfer process having the observed time dependence is a random walk in one dimension. In this case the Nd^{3+} ion in the excited metastable state is treated as a Frenkel exciton which can migrate to other sensitizer ions before becoming trapped at an activator site. The energy transfer rate for a random walk process can be expressed as the rate at which the exciton sample new sites multiplied by the fraction of total sites occupied by activators [10]. Using the expression for the sampling function for a one-dimensional lattice gives [11]

$$\omega_{sa} = (2/\pi)^{1/2} N_a \left[\tau_s^{-1} (R_0/R)^6\right]^{1/2} t^{-1/2}, \tag{9}$$

where it has been assumed that each step in the random walk takes place by an electric dipole–dipole interaction mechanism between ions separated by a distance R. The closest Nd ion separation in $NdAl_3(BO_3)_4$ crystals is 5.91 Å. Using this and the measured value of the energy transfer rate in eq. (9) gives a value of $R_0 = 7.2$ Å which is consistent with the theoretical predictions of eq. (7).

The third possibility that the observed energy transfer characteristics are due to trap-modulated energy migration in three dimensions can not be easily proven or disproven since any type of trap distribution necessary to fit the data can be postulated [12]. An important question is whether or not exciton motion restricted to one dimension is feasible in this type of crystal. The published crystal structure of $NdAl_3(BO_3)_4$ indicates that a Nd ion site has 6 nearest neighbor Nd ions in various crystallographic directions [3]. However, more recent structural measurements describe this crystal as having a two-dimensional layered structure [13]. The feasibility of a preferred migration direction must await publication of the details of this structure. It should be emphasized that theoretical models for fitting the TRS data are very sensitive to the time dependence of the proposed energy transfer mechanism and attempts to fit the data with two-dimensional or three-dimensional random walk models or with single-step higher order multipole processes were all unsuccessful.

The observed temperature dependence of the energy transfer rate can provide further information about the nature of the energy transfer mechanism and the role played by phonons at high temperatures. Several different processes can contribute to the increase in the transfer rate with increasing temperature. These include the increase in the spectral overlap integral, the increase in the number of phonons available to make up the mismatch between sensitizer and activator transitions ($\Delta E_{sa} \approx 12$ cm^{-1}), and the increase in population of higher energy sensitizer and activator levels which can take part in the transfer process [14]. For this case the first two types of processes were

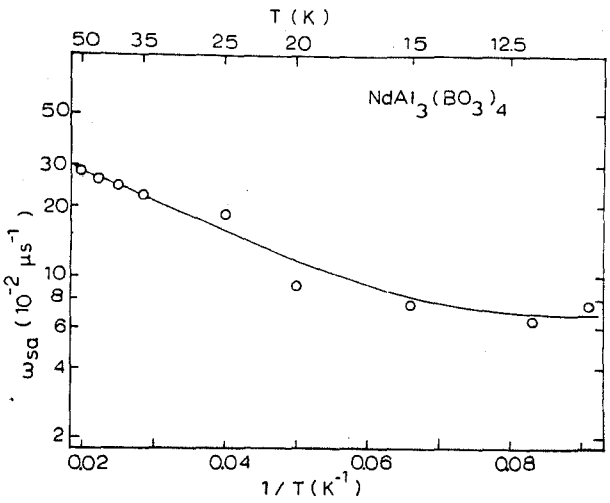

Fig. 6. Temperature dependence of the energy transfer rate. See text for explanation of the theoretical line.

found to be inconsistent with the data shown in fig. 6. The third mechanism can be applied to either single-step or multistep transfer. For a single-step process the expression for the energy transfer rate in eq. (6) would be written as the sum of transfer rates for each set of transitions weighted by the populations of the initial states of the transitions. The observed temperature dependence is not consistent with populating the first excited level of the ground state manifold of the activator, $E_{12} \approx 60\ \mathrm{cm}^{-1}$. A qualitative fit to the data shown in fig. 6 can be obtained assuming the important activation energy is $\Delta E_{ab} \approx 25\ \mathrm{cm}^{-1}$ which is needed to populate the higher crystal field component of the metastable state of the sensitizer. However, the room temperature spectrum shows that the b–1 transition is less intense than the a–1 transition and thus, energy transfer should not increase as the b level becomes populated from the a level [9].

The most consistent fit to the data is found from the one-dimensional random walk theory described by expressing eq. (9) as a sum over the thermally activated transitions involved in the migration. If the sum is simplified to include only the terms for the ground state and the first excited component the energy transfer rate is

$$\omega_{sa} = (2/\pi)^{1/2} N_a \left\{ \left[t_{H1}^{-1} \frac{1}{1 + e^{-\Delta E 12/kT}} \right]^{1/2} \right.$$

$$+\left[t_{H2}^{-1}\frac{e^{-\Delta E12/kT}}{1+e^{-\Delta E12/kT}}\right]^{1/2}\Bigg\}t^{-1/2}, \tag{10}$$

where t_{H1} and t_{H2} are the hopping times involving the two types of transitions. The good fit to the data shown by the solid line in fig. 6 was found with $\Delta E_{12} \approx 60$ cm^{-1}, $t_{H1}^{-1} \approx 0.075$ μs^{-1} and $t_{H2}^{-1} \approx 6.75$ μs^{-1}. Both the value of the activation energy and the fact that $t_{H2}^{-1} > t_{H1}^{-1}$ are consistent with spectral observations. The magnitude of t_{H1}^{-1} is consistent with the theoretical prediction $t_{H1}^{-1} = \tau_s^{-1}(R_0/R)^6$.

In summary, the energy transfer characteristics of NAB crystals are consistent with a one-dimensional random walk in which the hopping rate increases as the first excited component of the ground state multiplet becomes thermally activated. The diffusion coefficient at low temperatures is $D = \frac{1}{2}R^2/t_{H1} = 1.3 \times 10^{-10}$ cm^2 sec^{-1}. These characteristics are quite different from those found in other Nd^{3+}-doped crystals [15]. The differences may be associated with the different crystal structure of NAB which still must be clarified. It should be pointed out that the conventional approach to the study of energy transfer has been used in this investigation in that a phenomenological rate parameter model was utilized to obtain the primary characteristics of the transfer rate from the experimental data and secondary information was obtained from comparison with the predictions of standard theories. More sophisticated theories are now being developed which raise questions about some aspects of this conventional approach [16] but they are not yet established to the point where they can be used to analyze new data such as that obtained in this study.

Acknowledgements

This research was supported by the US Army Research Office. The authors are grateful to Professor G. Blasse for supplying the samples, and appreciate the helpful discussions with Dr. W. Zwicker concerning the crystal structure of NAB.

References

[1] S.R. Chinn, H.Y-P. Hong and J.A. Pierce, Laser Focus 12 (1976) 64.
[2] H.G. Danielmeyer, Festkörperprobleme (Advances in Solid State Physics), vol. 15, ed. H.J. Queisser (Pergamon/Vieweg, Braunschweig, 1975) p. 253.
[3] H.Y-P. Hong and K. Dwight, Mat. Res. Bull. 9 (1974) 1661.
[4] O. Jarchow, F. Lutz and K.H. Klaska, Diskussionstagung der Arbeitsgemeinschaft Kristallographie 19 (1972) 162.

[5] V.I. Bilak, I.I. Kuratev, N.I. Leonyuk, V.A. Pashkov, A.V. Pashkova, T.I. Timchenko and A.V. Shestakov, Sov. Phys. Dokl. 23 (1978) 299.
[6] H.D. Hattendorff, G. Huber and H.G. Danielmeyer, J. Phys. C11 (1978) 2399.
[7] M. Inokuti and F. Hirayama, J. Chem. Phys. 15 (1965) 1978.
[8] D.L. Dexter, J. Chem. Phys. 21 (1953) 836.
[9] S.R. Chinn and H.Y-P. Hong, Optics Comm. 15 (1975) 345.
[10] Z.G. Soos and R.C. Powell, Phys. Rev. B6 (1972) 4035.
[11] E.W. Montroll, Proc. Symp. Appl. Math. Am. Math. Soc. 16 (1963) 193.
[12] R.C. Powell and Z.G. Soos, Phys. Rev. B5 (1972) 1547.
[13] H.G. Danielmeyer, presented at the International Laser Symposium, 1979.
[14] M.J. Weber, Phys. Rev. B4 (1971) 2932.
[15] J.M. Flaherty and R.C. Powell, Phys. Rev. B19 (1979) 32;
L.D. Merkle and R.C. Powell, Phys. Rev. B20 (1979) 75;
M. Zokai, R.C. Powell, G.F. Imbusch and B. DiBartolo, J. Appl. Phys. 50 (1979) 5930;
D.K. Sardar and R.C. Powell, J. Appl. Phys. 51 (1980) 2829.
[16] D.L. Huber, Phys. Rev. B20 (1979) 2307, 5333;
K.K. Ghosh and D.L. Huber, J. Lumin. 21 (1980) 225;
K.K. Ghosh, J. Hagarty and D.L. Huber, Phys. Rev. B22 (1980) 2837.